https://doi.org/10.5028/jatm.v11.982 ORIGINAL PAPER

Research on Sliding Mode Method about Three-Dimensional Integrated Guidance and Control for Air-to-Ground Missile

Zhikai Wang[1], Jianwei Ma[1,2]*, Jiangtao Fu[1]

Wang ZK https://orcid.org/0000-0002-1692-2080
Ma JW https://orcid.org/0000-0003-4069-8880
Fu JT https://orcid.org/0000-0003-0698-3792

How to cite

Wang ZK; Ma JW; Fu JT (2019) Research on Sliding Mode Method about Three-Dimensional Integrated Guidance and Control for Air-to-Ground Missile. J Aerosp Technol Manag, 11: eXX19. https://doi.org/10.5028/jatm.v11.982

ABSTRACT: Based on adaptive sliding mode-control and back-stepping design method, an integrated guidance and control method with less calculation is proposed, which is designed for air-to-ground missile during the terminal course in three-dimensional space. The model of the control system with nonlinear and coupling is simplified, then the integrated guidance and control model in pitch and yaw channel is established. The coupling terms and modeling error between channels is considered as unknown bounded disturbance. An extended state observer is developed to estimate and compensate the unknown disturbance. In the design process, the block dynamic surface method is adopted, and the first order low pass filter is introduced to avoid the problem of differential explosion present in the traditional back-stepping design method during the process of differentiating virtual control variable. The Lyapunov stability theory is used to prove the stability of the system. Finally, in the case of nominal and positive and negative perturbations of model parameters, the simulation experiments are carried outto verify the effectiveness of the proposed IGC algorithm.

KEYWORDS: Integrated guidance and control, Adaptive back-stepping sliding mode, Dynamic surface, Air-to-ground missile, Extended state observer.

INTRODUCTION

The traditional design method of the missile guidance and control system is based on the idea of separation; the system is divided into fast loop (control loop) and slow loop (guidance loop). First the guidance loop is designed and the desired overload is obtained. After, in order to track the desired overload, the control loop is designed. During the terminal course, with the distance between the missile and the target becoming closer, the frequency of the guidance loop becomes faster, the coupling between the two loops becomes larger, thence it is difficult to design each subsystem separately, which always leads to a larger miss distance. At the moment, in order to achieve comprehensive index requirements, such as the angle changes slowly, the miss distance is as small as possible and the trajectory of the missile is relatively smooth.

It is necessary to exploit the synergistic relationship of guidance and control system. Hence such a design approach usually leads to excessive design iterations. As a result, the idea of IGC method is not to distinguish the guidance loop and control loop, taking into account the coupling relationship between the guidance loop and control loop as a whole (Shima *et al.* 2006; Shtessel and Tournes 2009; Liu *et al.* 2016). Further IGC generates the fin deflection commands according to the states of the

1.Henan University of Science and Technology – School of Information Engineering – Luoyang/Henan – China.
2.Henan University of Science and Technology – Henan Key Laboratory of Robot and Intelligent Systems – Luoyang/Henan – China.
***Correspondence author:** lymjw@163.com
Received: Dec. 1, 2017 | **Accepted:** Mar. 5, 2018
Section Editor: Luiz Martins-Filho

missile and the target relative by azimuth angle of the line-of-sight and the information of missile states. By the way, this can ensure that missile instability is avoided and the guidance accuracy is improved.

Many experts have done a lot of researches since the integrated guidance and control method was proposed. In the early paper, the method of integrated guidance and control is applied to the design of homing missiles (Yueh and Lin 1984; Mingzhe and Guangren 2008). Based on the linear quadratic optimal control theory, an optimal integrated guidance and control algorithm is designed for the stationary target. The design of nonlinear system usually requires linearization, and then the linear control methods are used. In the feedback linearization method, the nonlinear system is transformed into a linear system, which requires complicated numerical calculations (Menon and Ohlmeyer 2001). In the nonlinear optimal control method, Hamilton Jacobi Bellman (HJB) equation needs to be solved online, therefore complicated numerical calculations are also inevitable (Xin *et al.* 2006; Vaddi *et al.* 2009). To deal with the more complex models in three-dimensional space, the Riccati differential equation and extended linearization are used to design the IGC algorithm of homing missile (Evers *et al.* 1992; Menon and Ohlmeyer 1999). This method is suitable for complex systems. However, the problem of large online computation is still exited in this method.

As the missiles have features with nonlinear, strong coupling, disturbance uncertainty, parameter perturbation, in recent years the sliding mode control method has been widely used because of its fast response, insensitive of system parameters perturbation and external disturbance, robustness and simple algorithm design. It has also been widely used in the design of IGC of aircraft (Shamaghdari *et al.* 2015), missile (Zhu *et al.* 2013) and unmanned helicopter (Yamasaki *et al.* 2012). In the existing papers, most of them are designed in a single channel (Jegarkandi *et al.* 2015; Seyedipour *et al.* 2017), regardless of the coupling between channels. The use of observers to compensate for system uncertainty and disturbance can provide a better control effect, but the advantages of IGC method can't be fully exploited in three dimensions. Some papers design IGC algorithms in three dimensions (Yeh 2010; Song and Song 2016; Wang *et al.* 2016), but it is difficult to design the controller to the establishment of the model with a high order. When using the Slide-To-Turn (STT) method, the model can be established with lower order equation, because the roll channel is relatively stable and only the pitch and yaw channels are considered (Chao *et al.* 2014; Lee *et al.* 2016). However, as the process of designing the controller involves the matrix inversion, the calculation is relatively complex.

In this paper, an IGC algorithm is proposed, using STT method to attack the ground moving target during the terminal course in three-dimensional space for air-to-ground missile. The modeling error and coupling between pitch and yaw channel are treated as an unknown disturbance, and the disturbance with nonlinear uncertainty is estimated with the ESO and compensated in the controller through feedback. Fortunately, this model satisfies the so-called block low-triangular structure. Thus, the back-stepping method combined with adaptive proximity law sliding mode control is used to design a controller in this paper. The designed controller is simple and easy to achieve in actual system.

MOTION MODEL

The three-dimensional motion model of air-to-ground missile has features with complex nonlinear, strong coupling and parameter uncertain, which makes the design of the control system difficult. The model needed to be simplified in the actual design; generally the missile's three-dimensional guidance problem is divided into pitch plane and yaw plane. In this paper, we make the following assumptions about the integration model of air-to-ground missile:

- The rolling channel of missile is relatively stable, ignoring the missile's rolling motion.
- For one channel, the effect of coupling with the rest of the channels is considered as unknown bounded uncertainties.
- In the terminal course, the missile has no thrust, the speed of the missile and the target do not change.

Based on the above assumptions and considering Hou (2011), the pitch and yaw channel IGC model of the missile is established as follows.

MOTION MODEL IN PITCH

Taking the pitch channel as example, the vertical plane IGC model is established according to the relative motion relation of missile-target and the dynamic equation of the missile body.

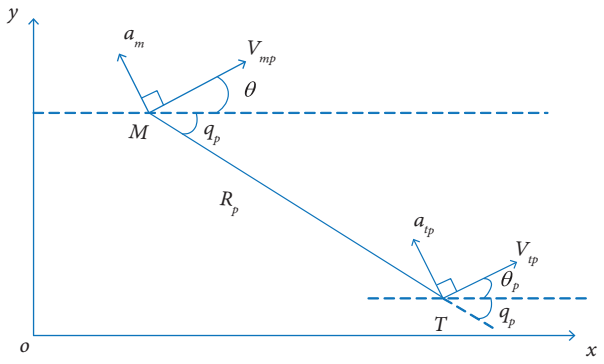

x, o, y: Ground coodinate axes

Figure 1. Missile-to-target relative in vertical plane.

In Fig. 1, M and T are the position of the missile and the target, where V_{mp} and V_{tp} are the speed of the missile and the target in the pitch plane, the θ and θ_{tp} respectively represent the flight path angle of the missile and target, the normal acceleration of the missile and the target in the pitch plane are respectively represented by a_m and a_{tp}, q_p is the azimuth angle of the line-of-sight, R_p is the distance of missile and target in the pitch plane. Define the angle q_p, angle θ_{tp} and angle θ above the baseline for positive and vice versa (Eq. 1).

$$\begin{cases} \dot{R}_p = V_{tp}\cos(\mathrm{q}_p - \theta_{tp}) - V_{mp}\cos(\mathrm{q}_p - \theta) \\ R_p\dot{q}_p = V_{mp}\sin(\mathrm{q}_p - \theta) - V_{tp}\sin(\mathrm{q}_p - \theta_{tp}) \\ V_{qp} = R_p\dot{q}_p \end{cases} \tag{1}$$

where V_{qp} is the line of sight rate, perpendicular to the line of missile-target. Equation 2 can be obtained:

$$\begin{cases} \ddot{q}_p = -2\dot{R}_p\dot{q}_p / R_p - a_m / R_p + \Delta q_p \\ \dot{V}_{qp} = -\dot{R}_p\dot{q}_p - a_m + R_p\Delta q_p \end{cases} \tag{2}$$

where, Δq_p is an unknown disturbance.

In this paper the following dynamic model of missile in pitch channel is adopted (Eq. 3) (Shima *et al.* 2006).

$$\begin{cases} \dot{\alpha} = \omega_z - \dfrac{1}{mv_p}(57.3qSC_y^{\alpha}\alpha - G\cos\theta) \\ \dot{\omega}_z = \dfrac{qSL}{I_z}(m_z^{\bar{\omega}_z}\dfrac{L}{v_p}\omega_z + 57.3m_z^{\alpha}\alpha + 57.3m_z^{\delta_z}\delta_z) \\ \dfrac{d\vartheta}{dt} = \omega_z \end{cases} \tag{3}$$

where α is the angle of attack, ω_z is the a is the pitch rate, m is the mass of the missile, G is the gravity of the missile, q is dynamic pressure, S is the feature area of the missile, L is the reference length of the missile, I_z is the moment of inertia around the pitch axis, δ_z is the elevator deflection, ϑ is the pitch angle, θ is the flight path angle, C_y^{α} is the rise lift coefficient corresponding to

the missile attack angle, $m_z^{\omega z}$, m_z^{α} and $m_z^{\delta z}$ respectively represent the pitch moment coefficient corresponding to ω_z, α and δ_z. The normal acceleration of the missile in pitch channel is as follows (Eq. 4):

$$a_m = \frac{57.3qSC_y^{\alpha}\alpha - G\cos(\theta)}{m} \tag{4}$$

According to the above analysis, the IGC model of the missile can be obtained as follows (Eq. 5):

$$\begin{cases} \dot{V}_{qp} = -\dot{R}_p\dot{q}_p - \dfrac{57.3qSC_y^{\alpha}\alpha - G\cos\theta}{m} + \Delta_1 \\ \dot{\alpha} = \omega_z - \dfrac{57.3qSC_y^{\alpha}\alpha - G\cos\theta}{mv_{mp}} + \Delta_2 \\ \dot{\omega}_z = \dfrac{57.3qSL(\mathrm{m}_z^{\alpha}\alpha + \mathrm{m}_z^{\delta_z}\delta_z)}{I_z} + \dfrac{qsl^2m_z^{\omega_z}\omega_z}{I_zv_{mp}} + \Delta_3 \end{cases} \tag{5}$$

where $\Delta_1, \Delta_2, \Delta_3$ are unknown bounded uncertainties.

The IGC model in pitch channel can be simplified as follows (Eq. 6):

$$\begin{cases} \dot{x}_1 = f_1(x_1) + x_2 + d_1 \\ \dot{x}_2 = f_2(x_2) + x_3 + d_2 \\ \dot{x}_3 = f_3(x_2, x_3) + b_pu_p + d_3 \end{cases} \tag{6}$$

where: $x_1 = \dfrac{v_{qp}}{-57.3qSC_y^{\alpha}/m}$, $x_2 = \alpha$, $x_3 = \omega_z$, $b_p = \dfrac{57.3qSLm_z^{\delta_z}}{I_z}$, $u_p = \delta_z$, $f_1(x_1) = -\dfrac{\dot{R}_p}{R_p}x_1 + \dfrac{G\cos\theta}{-57.3qSC_y^{\alpha}}$,

$f_2(x_2) = \dfrac{-57.3qSC_y^{\alpha}}{mv_{mp}}x_2 + \dfrac{G\cos\theta}{mv_{mp}}$ $f_3(x_2, x_3) = \dfrac{57.3qSLm_z^{\alpha}}{I_z}x_2 + \dfrac{qSL^2m_z^{\omega_z}}{I_zv_{mp}}$, $d_1 = \dfrac{\Delta_1}{-57.3qSC_y^{\alpha}/m}$, $d_2 = \Delta_2$, $d_3 = \Delta_3$.

MOTION MODEL IN YAW

Similarly, the yaw channel IGC model is established according to the relative motion in the yaw channel and the motion equation of the missile body.

The normal acceleration of the missile in yaw channel can be described as follows (Eq. 7):

$$a_z = \frac{57.3qSC_y^{\beta}\beta}{m} \tag{7}$$

The IGC model in yaw channel is established as follows (Eq. 8):

$$\begin{cases} \dot{V}_{qy} = -\dot{R}_y\dot{q}_y - \dfrac{57.3qSC_z^{\beta}\beta}{m} + \Delta_4 \\ \dot{\beta} = \omega_y + \dfrac{57.3qSC_z^{\beta}\beta}{mv_y} + \Delta_5 \\ \dot{\omega}_y = \dfrac{57.3qSL(\mathrm{m}_y^{\beta}\beta + \mathrm{m}_y^{\delta_y}\delta_y)}{I_y} + \dfrac{qSL^2m_y^{\omega_y}\omega_y}{I_yv_y} \end{cases} \tag{8}$$

where Δ_4, Δ_5, Δ_6 are unknown bounded uncertainties, R_y is the projection of distance between missile and target in yaw plane, v_y is the projection of missile speed V in the yaw plane, β is the sideslip angle of the missile, ω_y is yaw rate, I_y is the moment of inertia around the yaw axis, δ_y is the rudder deflection, C_z^{β} is the lateral force coefficient which corresponding to the missile sideslip angle β, m_y^{β}, $m_y^{\omega y}$, and $m_y^{\delta y}$ respectively represent the yaw moment coefficient corresponding to β, ω_y and δ_y.

The IGC model in yaw channel can be rewritten as follows (Eq. 9):

$$\begin{cases} \dot{x}_4 = f_4(x_4) + x_5 + d_4 \\ \dot{x}_5 = f_5(x_5) + x_6 + d_5 \\ \dot{x}_6 = f_6(x_5, x_6) + b_y u_y + d_6 \end{cases} \tag{9}$$

where:

$$x_4 = \frac{v_{qy}}{-57.3qSC_z^{\beta}/m},\ x_5 = \beta,\ x_6 = \omega_y,\ u_y = \delta_y,\ b = \frac{57.3qSLm_y^{\delta_y}}{I_y},\ d_4 = \frac{\Delta_4}{-57.3qSC_z^{\beta}/m},\ d_5 = \Delta_5,\ d_6 = \Delta_6,$$

$$f_4(x_4) = -\frac{\dot{R}_y}{R_y}x_5,\quad f_5(x_5) = \frac{57.3qSC_z^{\beta}}{mv_y}x_5\ \ f_6(x_5, x_6) = \frac{57.3qSLm_y^{\beta}}{I_y}x_2 + \frac{qSL^2m_y^{\omega_y}}{I_y v_y}.$$

EXTENDED STATE OBSERVER

The uncertainties of the system with nonlinear can be estimated by the extended state observer and compensate in the control system by feedback. In this paper, coupling between pitch and yaw channel, system parameters perturbation and modeling error are seen as unknown bounded uncertainties, which are estimated by extended state observers and treated as extend states. (Xia *et al.* 2011) The design principle of the extended state observer is illustrated by taking the first closed-loop subsystem of Eq. 6 as an example.

$$\dot{x}_1 = f_1(x_1) + x_2 + d_1 \tag{10}$$

In this system, d_1 is unknown uncertainty. The system (Eq. 10) can be described as follows (Eq. 11):

$$\begin{cases} \dot{x}_1 = f_1(x_1) + x_2 + x_{1d} \\ \dot{x}_{1d} = g_1(\mathrm{t}) \end{cases} \tag{11}$$

where x_{1d} is the extend state of d_1, $g_1(\mathrm{t})$ is the differential of extend state. The second-order extend state observer is designed as follows (Eq. 12):

$$\begin{cases} E_{11} = Z_{11} - x_1 \\ \dot{Z}_{11} = Z_{12} + f_1(x_1) - \gamma_{11}E_{11} + x_2 \\ \dot{Z}_{12} = -\gamma_{12}fal(E_{11}, \mu_1, \delta_1) \end{cases} \tag{12}$$

where Z_{11} and Z_{12} respectively represent the estimated values of state value x_1 and disturbance value d_1, E_{11} is state value error, γ_{11} and γ_{12} are the gain of ESO, μ_1 and δ_1 are the parameters of the ESO. The function *fal* is defined as follows (Eq. 13):

$$fal(E_{11}, \mu_1, \delta_1) = \begin{cases} |E_{11}|^{\mu_1}\,\mathrm{sgn}(E_{11}) & |E_{11}| > \delta_1 \\ E_{11}/\delta_1^{1-\mu_1} & |E_{11}| \le \delta_1 \end{cases} \tag{13}$$

The observation error of the ESO is defined as follows (Eq. 14):

$$E_{12} = Z_{12} - d_1 \tag{14}$$

The dynamic equation of observation error can be described as follows (Eq. 15):

$$\begin{cases} \dot{E}_{11} = E_{12} - \gamma_{11} E_{11} \\ \dot{E}_{12} = -g_1(\mathrm{t}) - \gamma_{12} fal(E_{11}, \mu_1, \delta_1) \end{cases} \tag{15}$$

The observer error is determined by the observer parameter γ_{11}, γ_{12}, μ_1, δ_1. By selecting the appropriate parameters, the observation values of the ESO x_1 and d_1 can converge to a small neighborhood of zero within a finite time.

According to a large number of numerical simulations experience, the selection of the observer parameters obey the following rules. For nonlinear function $fal(E_{11}, \mu_1, \delta_1)$, choosing $\mu_1 = 1/2^{n-1}$, $\delta_1 = h$, where n is the order of the observer, h is the integration step time of the numerical simulations. The selection of parameters γ_{11} and γ_{12} is related to h, usually the value of γ are chosen as follows: $\gamma_{11} = 1/h$, $\gamma_{11} = 1/3h^2$.

Based on the above design principle of ESO, ESO is designed for the remaining five subsystems of the closed loop system (Eq. 6) and the closed loop system (Eq. 9), and the state value and the disturbance value are estimated. Finally, we get the estimate values Z_{i1}, Z_{i2} respectively about system state value, E_{i1}, E_{i2} is the observer error. The parameters can be designed as γ_{i1}, γ_{i2}, μ_i, δ_i, $i = (1, 2, 3, 4, 5, 6)$.

IGC CONTROLLER DESIGN IN PITCH

Step 1

Considering the first subsystem of Eq. 6 (Eq. 16):

$$\dot{x}_1 = f_1(x_1) + x_2 + d_1 \tag{16}$$

Define x_{1c} as the command signal of the first subsystem in Eq. 6. In order to achieve the purpose of guidance, zero the line of sight angular velocity, that is $x_1 \to 0$. Define the subsystem tracking error as follows (Eq. 17).

$$e_1 = x_1 - x_{1c} \tag{17}$$

Then the dynamic error of the equation can be described as follows (Eq. 18):

$$\dot{e}_1 = f_1(x_1) + x_2 + d_1 - \dot{x}_{1c} \tag{18}$$

The estimated value Z_{12} of disturbance d_1 can be obtained by ESO, then, according to the ides of back-stepping design, the following virtual control value is designed (Eq. 19):

$$x_{2c} = -(k_1 e_1 + f_1(x_1) + Z_{12} - \dot{x}_{1c}) \tag{19}$$

The parameter k_1 is a positive constant that will be designed in controller.

Step 2

Considering the second subsystem of Eq. 6 (Eq. 20):

$$\dot{x}_2 = f_2(x_2) + x_3 + d_2 \tag{20}$$

Define the tracking error of the second subsystem in Eq. 6 as follows (Eq. 21):

$$e_2 = x_2 - x_{2c} \tag{21}$$

The dynamic error equation can be written as follows (Eq. 22):

$$\dot{e}_2 = f_2(x_2) + x_3 + d_2 - \dot{x}_{2c} \tag{22}$$

In the process of back-stepping design (Hwang and Tahk 2006), the derivative of the virtual control value will lead to differential explosion. In order to overcome this shortcoming, the first-order low-pass filter is designed by dynamic surface method, and the output of the filter $\bar{x}_{2c}$ is selected as the estimation of the input x_{2c}. The first-order low-pass filter is designed as follows (Eq. 23):

$$\begin{cases} \tau_1 \dot{\bar{x}}_{2c} + \bar{x}_{2c} = x_{2c} \\ \bar{x}_{2c}(0) = x_{2c}(0) \end{cases} \tag{23}$$

where τ_1 is the filter time constant. Define the filter error b_1 of virtual control value x_{2c} as follows (Eq. 24):

$$b_1 = \bar{x}_{2c} - x_{2c} \tag{24}$$

Then, the error dynamic equation can be described as follows (Eq. 25):

$$\dot{b}_1 = -b_1 / \tau_1 - \dot{x}_{2c} \tag{25}$$

The estimated value Z_{12} of disturbance d_2 can be obtained by ESO, then, according to the idea of back-stepping method, the following virtual control value is designed (Eq. 26):

$$x_{3c} = -(k_2 e_2 + f_2(x_2) + Z_{22} - \dot{x}_{2c} + e_2) \tag{26}$$

The parameter k_1 is a positive constant that will be designed in controller.

Step 3

Considering the third subsystem of Eq. 6 (Eq. 27):

$$\dot{x}_3 = f_3(x_2, x_3) + b_p u_p + d_3 \tag{27}$$

Define the tracking error of the second subsystem in Eq. 6 as follows (Eq. 28):

$$e_3 = x_3 - x_{3c} \tag{28}$$

In order to eliminate the tracking error between x_{3c} and x_3, slide-mode control method is adopted (Shtessel and Tournes 2009); define the sliding mode manifold as follows (Eq. 29):

$$s_1 = e_3 \tag{29}$$

The differential of S_1 can be obtained as follows (Eq. 30):

$$\dot{s}_1 = f_3(x_2, x_3) + b_p u_p + d_3 - \dot{x}_{3c} \tag{30}$$

Similarly, according to the design method of Step 2, the first-order low-pass filter can be described as follows (Eq. 31):

$$\begin{cases} \tau_2 \dot{\bar{x}}_{3c} + \bar{x}_{3c} = x_{3c} \\ \bar{x}_{3c}(0) = x_{3c}(0) \end{cases} \tag{31}$$

where τ_2 is the filter time constant. Define filtering error of virtual control value x_{3c} as follows (Eq. 32):

$$b_2 = \bar{x}_{3c} - x_{3c} \tag{32}$$

Then, the error dynamic equation can be described as follows (Eq. 33):

$$\dot{b}_2 = -b_2 / \tau_2 - \dot{x}_{3c} \tag{33}$$

The estimate value Z_{12} of disturbance d_2 can be obtained by ESO, and then the Eq. 30 can be rewritten as follows (Eq. 34):

$$\dot{s}_1 = f_3(x_2, x_3) + b_p u_p + Z_{32} - \dot{\bar{x}}_{3c} \tag{34}$$

In order to make the tracking error quickly converge to zero, proximity method with adaptive ability is selected, which differential as follows (Eq. 35):

$$\dot{s}_1 = -\frac{k_1 \left| \dot{R}_p \right|}{R_p} s_1 - \sigma_1 \operatorname{sgn}(s_1) \tag{35}$$

where $k_1 > 0$, $\sigma_1 > 0$.

With the change of the distance between the missile and the target R_p, the rata that switching function move to the sliding mode manifold is adjusted adaptively, so as to achieve the effect of weakening the buffeting (Eq. 36):

$$\hat{\sigma}_1 = r_1 \left| s_1 \right| \tag{36}$$

where $r_1 > 0$.

Define σ_1 as the estimate error (Eq. 37):

$$\tilde{\sigma}_1 = \sigma_1 - \hat{\sigma}_1 \tag{37}$$

Thus the control value δ_y is obtained as (Eq. 38):

$$\delta_y = -\frac{f_3(x_2, x_3) + Z_{32} - \dot{\bar{x}}_{3c} + \frac{k_1 \left| \dot{R}_p \right|}{R_p} s_1 \sigma_1 \operatorname{sgn}(s_1)}{b_p} \tag{38}$$

Finally, we get the IGC controller based on the ESO and back-stepping sliding mode. Equation 38 is the final control equation.

STABILITY ANALYSIS IN PITCH

Lemma 1: For a Lyapunov Function x_{2c}:[0, ∞)∈R, the solution of the inequality equation $\dot{V} \leq \alpha V$ is: $V_t \leq e^{\alpha(t-t0)}\ V(t_0)$

If α is a positive number, then $V(t)$ converges to zero in exponential form.

Define following Lyapunov function (Eq. 39):

$$V = \frac{1}{2}s_1^{\ 2} + \frac{1}{2}\tilde{\sigma}_1^{\ 2} + \frac{1}{2}b_1^{\ 2} + \frac{1}{2}e_1^{\ 2} + \frac{1}{2}b_2^{\ 2} + \frac{1}{2}e_2^{\ 2} \tag{39}$$

Set $V = V_1 + V_2$. Then (Eqs. 40 to 42):

$$V_1 = s_1^{\ 2} + \tilde{\sigma}_1^{\ 2} \tag{40}$$

$$\dot{V}_1 = s_1\dot{s}_1 + \frac{\tilde{\sigma}_1\dot{\tilde{\sigma}}_1}{r_1} = s_1[-\frac{k_1|\dot{R}_p|}{R_p}s_1 - \hat{\sigma}_1\,\mathrm{sgn}(s_1)] + (\sigma_1 - \hat{\sigma}_1)(-|s_1|) = -\frac{k_i|\dot{R}_p|}{R}s_1^2 - \hat{\sigma}_1 s_1\,\mathrm{sgn}(s_1) + \hat{\sigma}_1|s_1| - \sigma_1|s_{i1}| = -(\frac{k_1|\dot{R}_p|}{R_p}s_1^2 + \sigma_1|s_1|) \leq 0 \tag{41}$$

$$V_2 = \frac{1}{2}b_1^{\ 2} + \frac{1}{2}e_1^{\ 2} + \frac{1}{2}b_2^{\ 2} + \frac{1}{2}e_2^{\ 2} \tag{42}$$

Then the differential of equation can be obtained as (Eq. 43):

$$\dot{V}_2 = b_1\dot{b}_1 + e_1\dot{e}_1 + b_2\dot{b}_2 + e_2\dot{e}_2 \tag{43}$$

The third subsystem is closed-loop stable, according to the Lyapunov stability theory (Dong *et al.* 2016). Since the correlation variables and their derivation of the system (Eq. 6) are bounded, thus, there is a nonnegative continuous function η_1 satisfies $|x_{2c}| \leq \eta_1$, substituting Eq. 25 into Eq. 42, the following equation is obtained (Eq. 44):

$$|\dot{b}_1 + b_1/\tau_1| \leq \eta_1 \tag{44}$$

Combine Eq. 25 and Eq. 44, then (Eq. 45):

$$b_1\dot{b}_1 \leq \frac{-b_1^2}{\tau_1} + |b_1|\eta_1 \tag{45}$$

Combine Eq. 17, Eq. 19 and Eq. 21, then (Eq. 46):

$$\dot{e}_1 = -k_1e_1 + e_2 + b_1 + Z_{11} \tag{46}$$

According to Young inequality equation $ab \leq a^2/2 + b^2/2$, and then combining Eq. 45 and Eq. 46, the following equation is obtained (Eq. 47):

$$\begin{aligned} e_1\dot{e}_1 + b_1\dot{b}_1 &= -k_1e_1^2 + e_1e_2 + b_1e_1 + Z_{11}e_1 + b_1\dot{b}_1 \leq -k_1e_1^2 + e_1e_2 + e_1^2 + \frac{b_1^2}{4} + e_1^2 + \frac{Z_{11}^2}{4} - \frac{b_1^2}{\tau_1} + b_1^2 + \frac{\eta_1^2}{4} \\ &= -(k_1 - 2)e_1^2 + e_1e_2 + \frac{5}{4}b_1^2 + \frac{Z_{11}^2}{4} - \frac{b_1^2}{\tau_1} + \frac{\eta_1^2}{4} \end{aligned} \tag{47}$$

Similarly, considering Eqs. 22, 24, 26 and 33, and applying Young inequality equation, Eq. 47 can be rewritten as (Eq. 48):

$$e_2\dot{e}_2 + b_2\dot{b}_2 \le -(k_2-2)e_2^2 + e_2e_3 + \frac{5}{4}b_2^2 + \frac{Z_{21}^2}{4} - \frac{b_2^2}{\tau_2} + \frac{\eta_2^2}{4} \tag{48}$$

Combining Eq. 46 and Eq. 48, the following results can be obtained (Eq. 49):

$$\dot{V}_2 \le -\sum_{i=1}^{2}(k_i-2)e_i^2 + e_2e_3 + \sum_{j=1}^{2}(\frac{5}{4}b_j^2 + \frac{Z_{j1}}{4} - \frac{b_j^2}{\tau_j} + \frac{\eta_j}{4}) \tag{49}$$

By designing an appropriate control law makes e_3 converge to zero neighborhoods. In order to satisfy the form of Theorem 1, Eq. 49 can be expressed as follows (Eq. 50):

$$\dot{V}_2 \le -\kappa V_2 + c \tag{50}$$

Define κ and c as follows: $c = \sum_{i=1}^{2}(\frac{N_j^{\,2}}{4} + \frac{\eta_j^{\,2}}{4})$, $\kappa = 2\min\left\{(k_1-2),(k_2-2),\frac{5}{4}-\frac{1}{\tau_1},\frac{5}{4}-\frac{1}{\tau_2}\right\}$.

According to lemma 1 and Eq. 50, the following equation should be established (Eq. 51):

$$\dot{V}_2(t) \le V_2(0)e^{-\kappa t} + \frac{c}{\kappa} \le V_2(0) + \frac{c}{\kappa},\ \forall t \ge 0 \tag{51}$$

To sump up, according to Eq. 41 the third closed loop subsystem is proved to be stable based on Lyapunov stability theory. By designing the control law, the state tracking error e_3 can be converged to a neighborhood of zero, which can ensure that the first and the second subsystems of the system (Eq. 6) are semi-globally unanimous bounded, thus, the tracking error of the system converges, and the global stability of the closed-loop system is obtained.

IGC CONTROLLER DESIGN IN YAW

Similarly to the pitch channel, the controller in yaw channel can be designed.

STABILITY ANALYSIS IN YAW

According to the stability analysis method of the system (Eq. 6), the closed-loop system (Eq. 9) can be proved to be globally stable.

NUMERICAL SIMULATIONS

The effectiveness of the IGC algorithm was verified by comparing with Liu's paper in three-dimensional (Liu *et al.* 2015). Simulation experiments are done using Matlab/Simulink. The target in ground with a constant speed is taken as the attack object, and the numerical simulation is carried out according to the following initial conditions (Table 1).

The initial speed of the missile is 400 m/s, its velocity component in the pitch plane is $V_p = V_m cos(\varphi_v)$, and $V_y = V_m cos(\theta)$ is the velocity component of the missile in the yaw plane. The initial flight path angle $\theta_0 = -30°$, heading angle $\varphi_{v0} = 45°$, the initial value of the attack angle α_0, slide angle β_0 pitch angle rate ω_{z0} yaw angle rate ω_{y0} are all zero. The ground target moving

in the yaw channel, its speed components in the x-axis and y-axis are 15 m/s. The missile's aerodynamic coefficients and stability derivatives of the nominal conditions are chosen as: $m_z^a = -0.18$, $m_z^{\delta z} = -0.28$, $m_z^{\omega z} = -128$, $m_y^{\beta} = -0.365$, $m_y^{\delta y} = -0.14$, $c_z^{\beta} = -0.1358$, $c_z^{\delta y} = -0.257$, $c_y^a = 0.6$, $c_y^{\delta z} = -0.0257$, $L = 0.57$ m, $S = 0.253$ m^2.

In order to reduce the system chattering caused by the symbolic function in the simulation, the sigmoid function is introduced instead of the symbol function. Define sigmoid function as $sig(x) = 2/[\,1 + exp\,(-ax)] - 1$ where $a > 0$, which size is determined by the convergence speed of the function.

The parameters of the ESO are designed as: $\gamma_{11} = \gamma_{21} = \gamma_{31} = \gamma_{41} = \gamma_{51} = \gamma_{61} = 50$, $\gamma_{12} = \gamma_{22} = \gamma_{32} = \gamma_{42} = \gamma_{52} = \gamma_{62} = 500$, $\mu_1 = \mu_2 = \mu_3 = \mu_4 = \mu_5 = \mu_6 = 0.5$, $\delta_1 = \delta_2 = \delta_3 = \delta_4 = \delta_5 = \delta_6 = 0.005$.

The controller parameters are designed as: $k_1 = k_2 = 6$, $r_1 = r_2 = 0.2$.

Table 1. Initial state of missile and target.

Missile state	Value	Target state	Value
Initial position X_{m0}	0 m	Initial position X_{t0}	2000 m
Initial position Y_{m0}	2000 m	Initial position Y_{t0}	0 m
Initial position Z_{m0}	0 m	Initial position Z_{t0}	2000 m
Initial speed V_{m0}	400 m/s	Initial speed V_{t0}	70 m/s

The time constant of the filter in the dynamic surface method is designed as: $\tau_1 = \tau_2 = \tau_3 = \tau_4 = 0.01$.

Considering the random disturbances the missile suffered in the process of moving outside, $\Delta_i(t) = 0.3\sin(3t)$, $i = (1, 2, 3, 4, 5, 6)$, and some numerical simulation is carried out in the nominal case and the missile parameters were positive and negative. Due to space constraints in this paper, the following only shows the simulation results curves under the standard situation, and the simulation curves of the states and disturbances observed by ESO in pitch channel.

It can be seen from Fig. 2 that the ESO can make an accurate estimate of the uncertain disturbance (Fig. 3). In Liu's paper(2015) there was no estimate to the disturbance.

From Figs. 4 to 8, it can be seen that the changes of attack angle, sideslip angle, rudder deflection, elevator deflection are slow, deflection angles meet to the constraints condition, which no more than ±20°, therefore the result of the simulations satisfy the requirements of actual system. The angles of the missile state also change slowly in Liu's paper (2015). At the end of the simulation, Liu *et al.* (2015) encountered a big fluctuation. In this paper that problem was avoided.

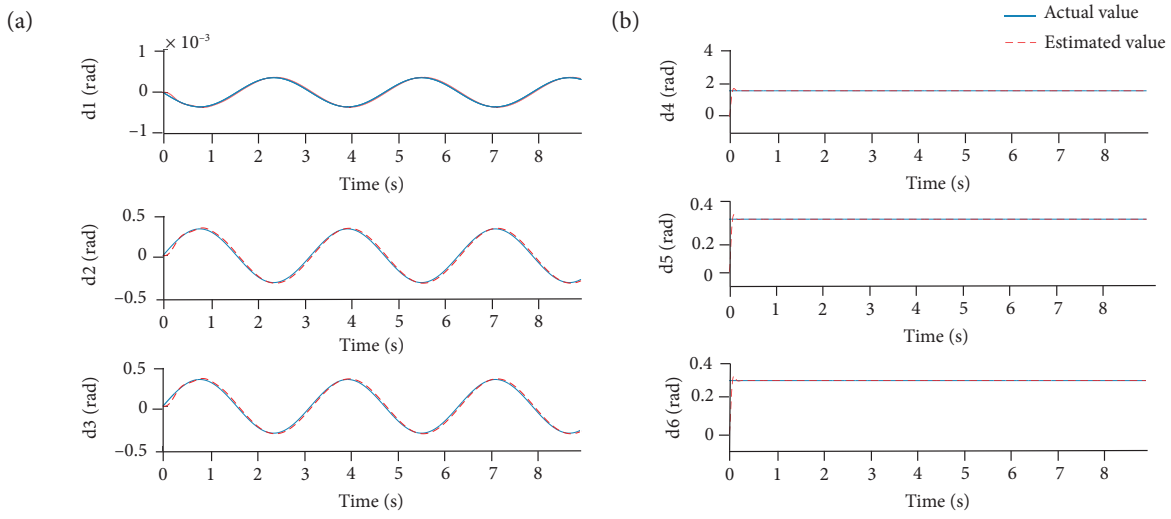

Figure 2. (a) Course of estimation of disturbance value (Pitch); (b) Course of estimation of disturbance value (Yaw).

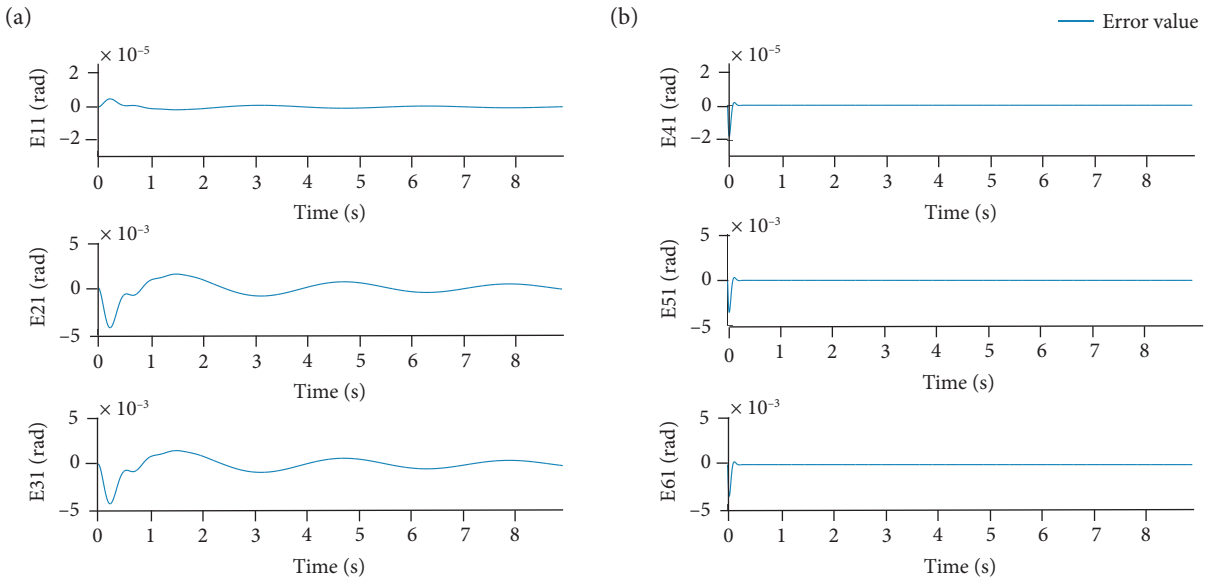

Figure 3. (a) Curves of estimation error of state value (Pitch); (b) Curves of estimation error of state value (Yaw).

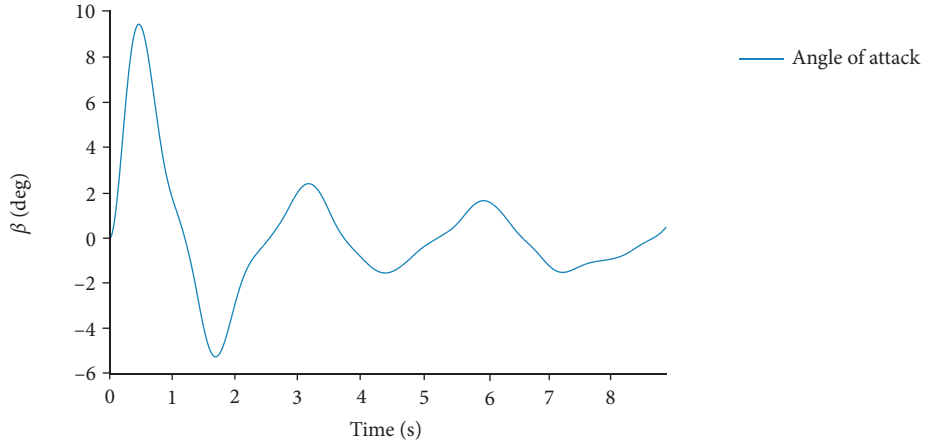

Figure 4. Curves of attack angle α.

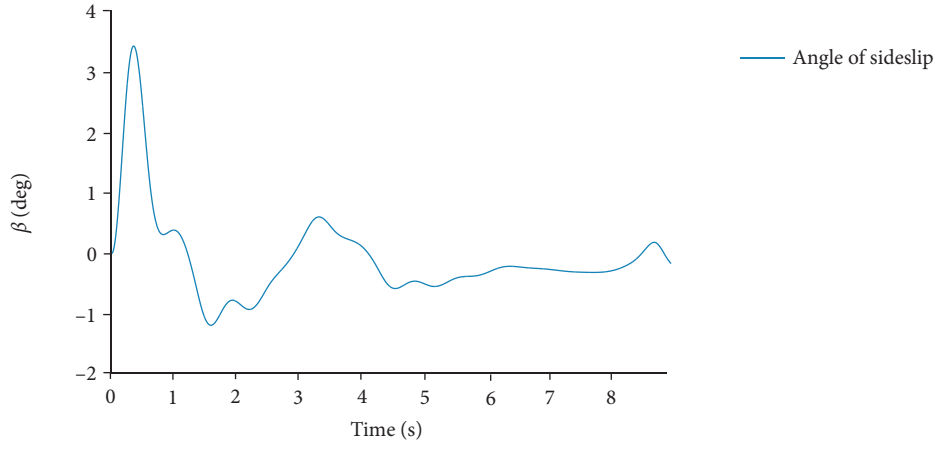

Figure 5. Curves of sideslip angle β.

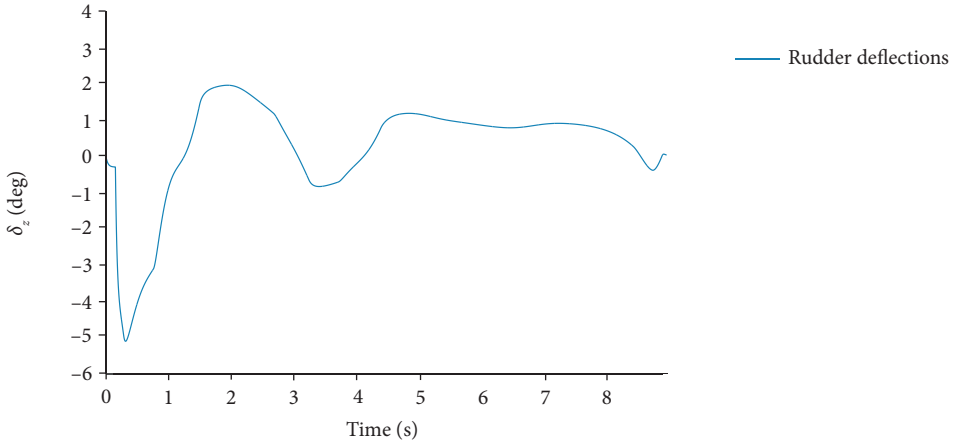

Figure 6. Curves of fin deflections δy.

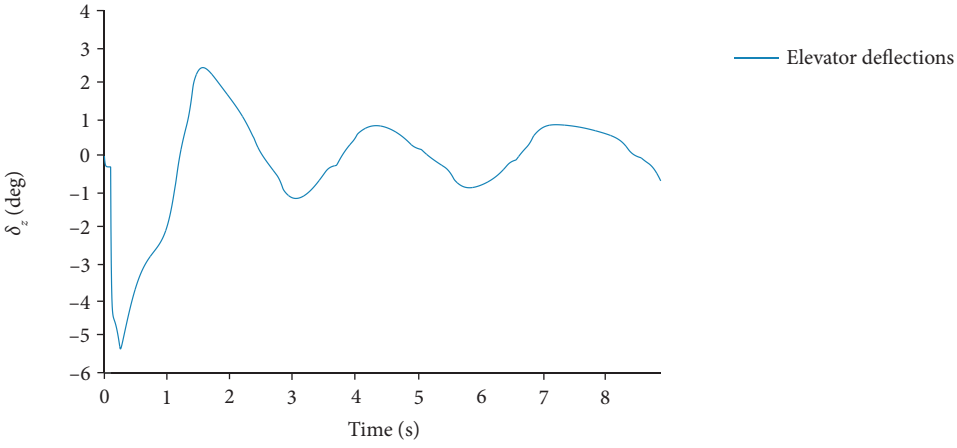

Figure 7. Curves of fin deflections δz.

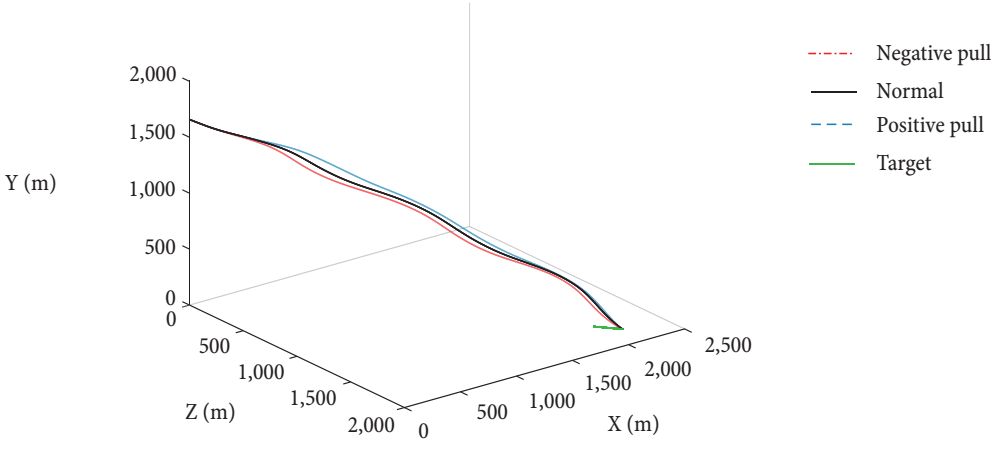

Figure 8. Missile and target trajectories.

In order to verify the robustness of the designed control algorithm, we pull the atmospheric density, aerodynamic force coefficient, and aerodynamic moment coefficient moment of inertia with a positive and negative direction, then, the numerical simulations are carried out.

It can be seen in Table 2 that, in the case of aerodynamic coefficients and stability derivatives without pull, the missile miss distance within 1 m; in the case of negative or positive pull of the aerodynamic coefficients and stability derivatives, the missed distance can reach less than 3 m. In Liu's paper (2015) the simulation was done without pull, and its missing distance is smaller. The missile trajectory changes little with the pull, and the missile can accurately hit the target, which shows the robustness of the designed controller.

Table 2. Instruction of parameter deviation.

Parameter	Positive pull	Normal	Negative pull
Atmospheric density	15%	0%	–15%
Aerodynamic force coefficient	15%	0%	–15%
Aerodynamic moment coefficient	30%	0%	–30%
Moment of inertia	10%	0%	–10%
Miss distance	1.962 m	0.7689 m	2.895 m

CONCLUSIONS

In this paper, an IGC model in pitch and yaw channel is designed for air-to-ground missile during the terminal course in three-dimensional space, considering the precise control of rolling channel. The back-stepping method and the adaptive proximity law sliding mode control method is adopted based on this model, moreover, the ESO is introduced to estimate the state value and disturbance value. The numerical simulations are carried out with the external disturbance and the pulled aerodynamic coefficients and stability derivatives. The numerical simulations results show that the designed controller has strong robustness and good guidance accuracy. In this paper, only the coupling of the pitch and yaw channels is taken into account in the modeling, and how to improve the controller in the case of the coupling of the rolling channel, which makes the application more general and will become the next research.

FUNDING

National Natural Science Fund of China
Grant No: U1604146
Science and Technology Project of Henan Province
Grant No: 172102410071

AUTHOR'S CONTRIBUTION

Conceptualization, Wang ZK; Methodology, Wang ZK; Investigation, Wang ZK, Ma JW; Writing – Original Draft, Wang ZK, Ma JW and Fu JT; Writing – Review and Editing, Wang ZK and Fu JT; Funding Acquisition, Ma JW; Resources, Ma JW and Fu JT; Supervision, Ma JW.

REFERENCES

Chao T, Wang SY, Tian GB, Yang M (2014) Integrated guidance and control with terminal impact angular constraint for bank to turn flight vehicle. Presented at: 33rd Chinese Control Conference; Nanjing, China. http://doi.org/10.1109/ChiCC.2014.6896707

Dong CY, Cheng HY, Wang Q (2016) Backstepping sliding mode control for integrated guidance and control design based on active disturbance rejection. Systems Engineering and Electronics 37(7):1604-1610.

Hou MZ (2011) Integrated guidance and control for homing missiles (PhD Dissertation). Politics of R&D; p. 22-34. Harbin: Harbin Institute of Technology. In Chinese.

Hwang TW, Tahk MJ (2006) Integrated backstepping design of missile guidance and control with robust disturbance observer. Presented at: SICE-ICASE International Joint Conference; Busan, Korea. http://doi.org/10.1109/SICE.2006.314847

Jegarkandi MF, Ashrafifar A, Mohsenipour R (2015) Adaptive integrated guidance and fault tolerant control using back-stepping and sliding mode. J International Journal of Aerospace Engineering 2015:11365-11155. http://dx.doi.org/10.1155/2015/253478

Evers JH, Cloutier JR, Lin CF, Yueh WR, Wang Q (1992) Application of integrated guidance and control schemes to a precision guided missile. Presented at: 1992 American Control Conference; Chicago, USA. http://doi.org/10.23919/ACC.1992.4792745

Lee Y, Kim Y, Moon G, Jun BE (2016) Sliding-mode-based missile-integrated attitude control schemes considering velocity change. J Journal of Guidance, Control, and Dynamics 39(3):423-436. https://doi.org/10.2514/1.G001416

Liu MY, Liu XL, Li ZJ (2015) Guidance and control integrated design and simulation of air-to-surface miniature missile. J Computer Simulation 32(3):81-85. http://doi.org/10.3969/j.issn.1006-9348.2015.03.018

Liu X, Liu Z, Shan J, Sun H (2016) Anti disturbance autopilot design for missile system via finite integral sliding mode control method and nonlinear disturbance observer technique. Translations of the Institute of Measurement and Control 38(6):693-700. https://doi.org/10.1177/0142331215603793

Menon PK, Ohlmeyer EJ (1999) Integrated design of agile missile guidance and control systems. Presented at: 7th Mediterranean Conference on Control and Automation; Haifa, Israel.

Menon PK, Ohlmeyer EJ (2001) Integrated design of agile missile guidance and autopilot systems. Control Engineering Practice 9(10):1095-1106. https://doi.org/10.1016/S0967-0661(01)00082-X

Mingzhe H, Guargren D (2008) Integrated guidance and control of homing missiles against ground fixed targets. J Chinese Journal Of Aeronautics 21(2):162-168. http://doi.org/10.1016/S1000-9361(08)60021-7

Seyedipour SH, Jegarkandi MF, Shamaghdari S (2017) Nonlinear integrated guidance and control based on adaptive back-stepping scheme. Aircraft Engineering and Aerospace Technology 89(3):415-424. https://doi.org/10.1108/AEAT-12-2014-0209

Shamaghdari S, Nikravesh SKY, Haeri M (2015) Integrated guidance and control of elastic flight vehicle based on robust MPC. International Journal of Robust and Nonlinear Control 25(12):2608-2630. https://doi.org/10.1002/rnc.3215

Shima T, Idan M, Golan OM (2006) Sliding-mode control for integrated missile autopilot guidance. Journal of Guidance, Control, and Dynamics 29(2):250-260. https://doi.org/10.2514/1.14951

Shtessel YB, Tournes CH (2009) Integrated higher-order sliding mode guidance and autopilot for dual-control missiles. Journal of Guidance Control and Dynamics 32(1):79-94. https://doi.org/10.2514/1.36961

Song J, Song S (2016) Three-dimensional guidance law based on adaptive integral sliding mode control. Chinese Journal of Aeronautics 29(1):202-214. https://doi.org/10.1016/j.cja.2015.12.012

Vaddi SS, Menon PK, Ohlmeyer EJ (2009) Numerical state-dependent Riccati equation approach for missile integrated guidance control. Journal of Guidance, Control, and Dynamics 32(2):699-703. https://doi.org/10.2514/1.34291

Wang JH, Liu LU, Zhao T, Tang GJ (2016) Integrated guidance and control for hypersonic vehicles in dive phase with multiple constraints. Aerospace Science and Technology 53(6):103-115. https://doi.org/10.1016/j.ast.2016.03.019

Xia YQ, Zhu Z, Fu MY, Wang S (2011) Attitude tracking of rigid spacecraft with bounded disturbances. IEEE Trans on Industrial Electronics 58(2):647-659. http://doi.org/10.1109/TIE.2010.2046611

Xin M, Balakrishnan SN, Ohlmeyer EJ (2006) Integrated guidance and control of missiles with θ-D method. IEEE Transactions on Control Systems Technology 14(6):981-992. http://doi.org/10.1109/TCST.2006.876903

Yamasaki T, Balakrishnan SN, Takano H (2012) Integrated guidance and autopilot design for a chasing UAV via high-order sliding modes. Journal of the Franklin Institute 349(2):531-558. https://doi.org/10.1016/j.jfranklin.2011.08.004

Yeh FK (2010) Design of nonlinear terminal guidance/autopilot controller for missiles with pulse type input devices. Asian Journal of Control 12(3):399-412. https://doi.org/10.1002/asjc.196

Yueh WR, Lin CF (1984) Optimal controller for homing missile. Presented at: 1984 American Control Conference; San Diego, USA.

Zhu Z, Xu D, Liu JM, Xia Y (2013) Missile guidance law based on extended state observe. IEEE Transactions on Industrial Electronics 60(12):5882-5891. http://doi.org/10.1109/TIE.2012.2232254